

Search for Flavor-Changing Neutral-Current Charm Decays

The *BABAR* Collaboration

October 5, 2018

Abstract

We search for rare FCNC charm decays of the form $X_c^+ \rightarrow h^+ \ell^+ \ell'^-$, where X_c^+ is a charm hadron, h is a pion, kaon or proton, and $\ell^{(\prime)}$ is an electron or a muon. In the pion and kaon modes, we study both D^+ and D_s^+ decays, while in the proton modes we study Λ_c^+ decays. Based on a data sample of 288 fb^{-1} of e^+e^- collisions collected by *BABAR*, we set preliminary 90% confidence level limits between 4 to 40×10^{-6} for the branching fractions of the different decay modes. For most decay modes, our analysis provides a significant improvement over previous results.

Submitted to the 33rd International Conference on High-Energy Physics, ICHEP 06,
26 July—2 August 2006, Moscow, Russia.

Stanford Linear Accelerator Center, Stanford University, Stanford, CA 94309

Work supported in part by Department of Energy contract DE-AC03-76SF00515.

The BABAR Collaboration,

B. Aubert, R. Barate, M. Bona, D. Boutigny, F. Couderc, Y. Karyotakis, J. P. Lees, V. Poireau,
V. Tisserand, A. Zghiche

*Laboratoire de Physique des Particules, IN2P3/CNRS et Université de Savoie, F-74941 Annecy-Le-Vieux,
France*

E. Grauges

Universitat de Barcelona, Facultat de Física, Departament ECM, E-08028 Barcelona, Spain

A. Palano

Università di Bari, Dipartimento di Fisica and INFN, I-70126 Bari, Italy

J. C. Chen, N. D. Qi, G. Rong, P. Wang, Y. S. Zhu

Institute of High Energy Physics, Beijing 100039, China

G. Eigen, I. Ofte, B. Stugu

University of Bergen, Institute of Physics, N-5007 Bergen, Norway

G. S. Abrams, M. Battaglia, D. N. Brown, J. Button-Shafer, R. N. Cahn, E. Charles, M. S. Gill,
Y. Groysman, R. G. Jacobsen, J. A. Kadyk, L. T. Kerth, Yu. G. Kolomensky, G. Kukartsev, G. Lynch,
L. M. Mir, T. J. Orimoto, M. Pripstein, N. A. Roe, M. T. Ronan, W. A. Wenzel

Lawrence Berkeley National Laboratory and University of California, Berkeley, California 94720, USA

P. del Amo Sanchez, M. Barrett, K. E. Ford, A. J. Hart, T. J. Harrison, C. M. Hawkes, S. E. Morgan,
A. T. Watson

University of Birmingham, Birmingham, B15 2TT, United Kingdom

T. Held, H. Koch, B. Lewandowski, M. Pelizaeus, K. Peters, T. Schroeder, M. Steinke
Ruhr Universität Bochum, Institut für Experimentalphysik 1, D-44780 Bochum, Germany

J. T. Boyd, J. P. Burke, W. N. Cottingham, D. Walker

University of Bristol, Bristol BS8 1TL, United Kingdom

D. J. Asgeirsson, T. Cuhadar-Donszelmann, B. G. Fulsom, C. Hearty, N. S. Knecht, T. S. Mattison,
J. A. McKenna

University of British Columbia, Vancouver, British Columbia, Canada V6T 1Z1

A. Khan, P. Kyberd, M. Saleem, D. J. Sherwood, L. Teodorescu

Brunel University, Uxbridge, Middlesex UB8 3PH, United Kingdom

V. E. Blinov, A. D. Bukin, V. P. Druzhinin, V. B. Golubev, A. P. Onuchin, S. I. Serednyakov,
Yu. I. Skovpen, E. P. Solodov, K. Yu Todyshev

Budker Institute of Nuclear Physics, Novosibirsk 630090, Russia

D. S. Best, M. Bondioli, M. Bruinsma, M. Chao, S. Curry, I. Eschrich, D. Kirkby, A. J. Lankford, P. Lund,
M. Mandelkern, R. K. Mommsen, W. Roethel, D. P. Stoker

University of California at Irvine, Irvine, California 92697, USA

S. Abachi, C. Buchanan

University of California at Los Angeles, Los Angeles, California 90024, USA

S. D. Foulkes, J. W. Gary, O. Long, B. C. Shen, K. Wang, L. Zhang
University of California at Riverside, Riverside, California 92521, USA

H. K. Hadavand, E. J. Hill, H. P. Paar, S. Rahatlou, V. Sharma
University of California at San Diego, La Jolla, California 92093, USA

J. W. Berryhill, C. Campagnari, A. Cunha, B. Dahmes, T. M. Hong, D. Kovalskyi, J. D. Richman
University of California at Santa Barbara, Santa Barbara, California 93106, USA

T. W. Beck, A. M. Eisner, C. J. Flacco, C. A. Heusch, J. Kroseberg, W. S. Lockman, G. Nesom, T. Schalk,
B. A. Schumm, A. Seiden, P. Spradlin, D. C. Williams, M. G. Wilson
University of California at Santa Cruz, Institute for Particle Physics, Santa Cruz, California 95064, USA

J. Albert, E. Chen, A. Dvoretzkii, F. Fang, D. G. Hitlin, I. Narsky, T. Piatenko, F. C. Porter, A. Ryd,
A. Samuel
California Institute of Technology, Pasadena, California 91125, USA

G. Mancinelli, B. T. Meadows, K. Mishra, M. D. Sokoloff
University of Cincinnati, Cincinnati, Ohio 45221, USA

F. Blanc, P. C. Bloom, S. Chen, W. T. Ford, J. F. Hirschauer, A. Kreisel, M. Nagel, U. Nauenberg,
A. Olivas, W. O. Ruddick, J. G. Smith, K. A. Ulmer, S. R. Wagner, J. Zhang
University of Colorado, Boulder, Colorado 80309, USA

A. Chen, E. A. Eckhart, A. Soffer, W. H. Toki, R. J. Wilson, F. Winklmeier, Q. Zeng
Colorado State University, Fort Collins, Colorado 80523, USA

D. D. Altenburg, E. Feltresi, A. Hauke, H. Jasper, J. Merkel, A. Petzold, B. Spaan
Universität Dortmund, Institut für Physik, D-44221 Dortmund, Germany

T. Brandt, V. Klose, H. M. Lacker, W. F. Mader, R. Nogowski, J. Schubert, K. R. Schubert, R. Schwierz,
J. E. Sundermann, A. Volk
Technische Universität Dresden, Institut für Kern- und Teilchenphysik, D-01062 Dresden, Germany

D. Bernard, G. R. Bonneaud, E. Latour, Ch. Thiebaux, M. Verderi
Laboratoire Leprince-Ringuet, CNRS/IN2P3, Ecole Polytechnique, F-91128 Palaiseau, France

P. J. Clark, W. Gradl, F. Muheim, S. Playfer, A. I. Robertson, Y. Xie
University of Edinburgh, Edinburgh EH9 3JZ, United Kingdom

M. Andreotti, D. Bettoni, C. Bozzi, R. Calabrese, G. Cibinetto, E. Luppi, M. Negrini, A. Petrella,
L. Piemontese, E. Prencipe
Università di Ferrara, Dipartimento di Fisica and INFN, I-44100 Ferrara, Italy

F. Anulli, R. Baldini-Ferrolì, A. Calcaterra, R. de Sangro, G. Finocchiaro, S. Pacetti, P. Patteri,
I. M. Peruzzi,¹ M. Piccolo, M. Rama, A. Zallo
Laboratori Nazionali di Frascati dell'INFN, I-00044 Frascati, Italy

¹Also with Università di Perugia, Dipartimento di Fisica, Perugia, Italy

A. Buzzo, R. Capra, R. Contri, M. Lo Vetere, M. M. Macri, M. R. Monge, S. Passaggio, C. Patrignani,
E. Robutti, A. Santroni, S. Tosi

Università di Genova, Dipartimento di Fisica and INFN, I-16146 Genova, Italy

G. Brandenburg, K. S. Chaisanguanthum, M. Morii, J. Wu

Harvard University, Cambridge, Massachusetts 02138, USA

R. S. Dubitzky, J. Marks, S. Schenk, U. Uwer

Universität Heidelberg, Physikalisches Institut, Philosophenweg 12, D-69120 Heidelberg, Germany

D. J. Bard, W. Bhimji, D. A. Bowerman, P. D. Dauncey, U. Egede, R. L. Flack, J. A. Nash,
M. B. Nikolich, W. Panduro Vazquez

Imperial College London, London, SW7 2AZ, United Kingdom

P. K. Behera, X. Chai, M. J. Charles, U. Mallik, N. T. Meyer, V. Ziegler

University of Iowa, Iowa City, Iowa 52242, USA

J. Cochran, H. B. Crawley, L. Dong, V. Eyges, W. T. Meyer, S. Prell, E. I. Rosenberg, A. E. Rubin

Iowa State University, Ames, Iowa 50011-3160, USA

A. V. Gritsan

Johns Hopkins University, Baltimore, Maryland 21218, USA

A. G. Denig, M. Fritsch, G. Schott

Universität Karlsruhe, Institut für Experimentelle Kernphysik, D-76021 Karlsruhe, Germany

N. Arnaud, M. Davier, G. Grosdidier, A. Höcker, F. Le Diberder, V. Lepeltier, A. M. Lutz, A. Oyanguren,
S. Pruvot, S. Rodier, P. Roudeau, M. H. Schune, A. Stocchi, W. F. Wang, G. Wormser

*Laboratoire de l'Accélérateur Linéaire, IN2P3/CNRS et Université Paris-Sud 11, Centre Scientifique
d'Orsay, B.P. 34, F-91898 ORSAY Cedex, France*

C. H. Cheng, D. J. Lange, D. M. Wright

Lawrence Livermore National Laboratory, Livermore, California 94550, USA

C. A. Chavez, I. J. Forster, J. R. Fry, E. Gabathuler, R. Gamet, K. A. George, D. E. Hutchcroft,
D. J. Payne, K. C. Schofield, C. Touramanis

University of Liverpool, Liverpool L69 7ZE, United Kingdom

A. J. Bevan, F. Di Lodovico, W. Menges, R. Sacco

Queen Mary, University of London, E1 4NS, United Kingdom

G. Cowan, H. U. Flaecher, D. A. Hopkins, P. S. Jackson, T. R. McMahon, S. Ricciardi, F. Salvatore,
A. C. Wren

*University of London, Royal Holloway and Bedford New College, Egham, Surrey TW20 0EX, United
Kingdom*

D. N. Brown, C. L. Davis

University of Louisville, Louisville, Kentucky 40292, USA

J. Allison, N. R. Barlow, R. J. Barlow, Y. M. Chia, C. L. Edgar, G. D. Lafferty, M. T. Naisbit,
J. C. Williams, J. I. Yi

University of Manchester, Manchester M13 9PL, United Kingdom

C. Chen, W. D. Hulsbergen, A. Jawahery, C. K. Lae, D. A. Roberts, G. Simi

University of Maryland, College Park, Maryland 20742, USA

G. Blaylock, C. Dallapiccola, S. S. Hertzbach, X. Li, T. B. Moore, S. Saremi, H. Staengle

University of Massachusetts, Amherst, Massachusetts 01003, USA

R. Cowan, G. Sciolla, S. J. Sekula, M. Spitznagel, F. Taylor, R. K. Yamamoto

*Massachusetts Institute of Technology, Laboratory for Nuclear Science, Cambridge, Massachusetts 02139,
USA*

H. Kim, S. E. McLachlin, P. M. Patel, S. H. Robertson

McGill University, Montréal, Québec, Canada H3A 2T8

A. Lazzaro, V. Lombardo, F. Palombo

Università di Milano, Dipartimento di Fisica and INFN, I-20133 Milano, Italy

J. M. Bauer, L. Cremaldi, V. Eschenburg, R. Godang, R. Kroeger, D. A. Sanders, D. J. Summers,
H. W. Zhao

University of Mississippi, University, Mississippi 38677, USA

S. Brunet, D. Côté, M. Simard, P. Taras, F. B. Viaud

Université de Montréal, Physique des Particules, Montréal, Québec, Canada H3C 3J7

H. Nicholson

Mount Holyoke College, South Hadley, Massachusetts 01075, USA

N. Cavallo,² G. De Nardo, F. Fabozzi,³ C. Gatto, L. Lista, D. Monorchio, P. Paolucci, D. Piccolo,
C. Sciacca

Università di Napoli Federico II, Dipartimento di Scienze Fisiche and INFN, I-80126, Napoli, Italy

M. A. Baak, G. Raven, H. L. Snoek

*NIKHEF, National Institute for Nuclear Physics and High Energy Physics, NL-1009 DB Amsterdam, The
Netherlands*

C. P. Jessop, J. M. LoSecco

University of Notre Dame, Notre Dame, Indiana 46556, USA

T. Allmendinger, G. Benelli, L. A. Corwin, K. K. Gan, K. Honscheid, D. Hufnagel, P. D. Jackson,
H. Kagan, R. Kass, A. M. Rahimi, J. J. Regensburger, R. Ter-Antonyan, Q. K. Wong

Ohio State University, Columbus, Ohio 43210, USA

N. L. Blount, J. Brau, R. Frey, O. Igonkina, J. A. Kolb, M. Lu, R. Rahmat, N. B. Sinev, D. Strom,
J. Strube, E. Torrence

University of Oregon, Eugene, Oregon 97403, USA

²Also with Università della Basilicata, Potenza, Italy

³Also with Università della Basilicata, Potenza, Italy

A. Gaz, M. Margoni, M. Morandin, A. Pompili, M. Posocco, M. Rotondo, F. Simonetto, R. Stroili, C. Voci
Università di Padova, Dipartimento di Fisica and INFN, I-35131 Padova, Italy

M. Benayoun, H. Briand, J. Chauveau, P. David, L. Del Buono, Ch. de la Vaissière, O. Hamon,
B. L. Hartfiel, M. J. J. John, Ph. Leruste, J. Malcès, J. Ocariz, L. Roos, G. Therin
*Laboratoire de Physique Nucléaire et de Hautes Energies, IN2P3/CNRS, Université Pierre et Marie
Curie-Paris6, Université Denis Diderot-Paris7, F-75252 Paris, France*

L. Gladney, J. Panetta
University of Pennsylvania, Philadelphia, Pennsylvania 19104, USA

M. Biasini, R. Covarelli
Università di Perugia, Dipartimento di Fisica and INFN, I-06100 Perugia, Italy

C. Angelini, G. Batignani, S. Bettarini, F. Bucci, G. Calderini, M. Carpinelli, R. Cenci, F. Forti,
M. A. Giorgi, A. Lusiani, G. Marchiori, M. A. Mazur, M. Morganti, N. Neri, E. Paoloni, G. Rizzo,
J. J. Walsh
Università di Pisa, Dipartimento di Fisica, Scuola Normale Superiore and INFN, I-56127 Pisa, Italy

M. Haire, D. Judd, D. E. Wagoner
Prairie View A&M University, Prairie View, Texas 77446, USA

J. Biesiada, N. Danielson, P. Elmer, Y. P. Lau, C. Lu, J. Olsen, A. J. S. Smith, A. V. Telnov
Princeton University, Princeton, New Jersey 08544, USA

F. Bellini, G. Cavoto, A. D’Orazio, D. del Re, E. Di Marco, R. Faccini, F. Ferrarotto, F. Ferroni,
M. Gaspero, L. Li Gioi, M. A. Mazzoni, S. Morganti, G. Piredda, F. Polci, F. Safai Tehrani, C. Voena
Università di Roma La Sapienza, Dipartimento di Fisica and INFN, I-00185 Roma, Italy

M. Ebert, H. Schröder, R. Waldi
Universität Rostock, D-18051 Rostock, Germany

T. Adye, N. De Groot, B. Franek, E. O. Olaiya, F. F. Wilson
Rutherford Appleton Laboratory, Chilton, Didcot, Oxon, OX11 0QX, United Kingdom

R. Aleksan, S. Emery, A. Gaidot, S. F. Ganzhur, G. Hamel de Monchenault, W. Kozanecki, M. Legendre,
G. Vasseur, Ch. Yèche, M. Zito
DSM/Daphnia, CEA/Saclay, F-91191 Gif-sur-Yvette, France

X. R. Chen, H. Liu, W. Park, M. V. Purohit, J. R. Wilson
University of South Carolina, Columbia, South Carolina 29208, USA

M. T. Allen, D. Aston, R. Bartoldus, P. Bechtle, N. Berger, R. Claus, J. P. Coleman, M. R. Convery,
M. Cristinziani, J. C. Dingfelder, J. Dorfan, G. P. Dubois-Felsmann, D. Dujmic, W. Dunwoodie,
R. C. Field, T. Glanzman, S. J. Gowdy, M. T. Graham, P. Grenier,⁴ V. Halyo, C. Hast, T. Hryn’ova,
W. R. Innes, M. H. Kelsey, P. Kim, D. W. G. S. Leith, S. Li, S. Luitz, V. Luth, H. L. Lynch,
D. B. MacFarlane, H. Marsiske, R. Messner, D. R. Muller, C. P. O’Grady, V. E. Ozcan, A. Perazzo,
M. Perl, T. Pulliam, B. N. Ratcliff, A. Roodman, A. A. Salnikov, R. H. Schindler, J. Schwiening,
A. Snyder, J. Stelzer, D. Su, M. K. Sullivan, K. Suzuki, S. K. Swain, J. M. Thompson, J. Va’vra, N. van

⁴Also at Laboratoire de Physique Corpusculaire, Clermont-Ferrand, France

Bakel, M. Weaver, A. J. R. Weinstein, W. J. Wisniewski, M. Wittgen, D. H. Wright, A. K. Yarritu, K. Yi,
C. C. Young

Stanford Linear Accelerator Center, Stanford, California 94309, USA

P. R. Burchat, A. J. Edwards, S. A. Majewski, B. A. Petersen, C. Roat, L. Wilden

Stanford University, Stanford, California 94305-4060, USA

S. Ahmed, M. S. Alam, R. Bula, J. A. Ernst, V. Jain, B. Pan, M. A. Saeed, F. R. Wappler, S. B. Zain

State University of New York, Albany, New York 12222, USA

W. Bugg, M. Krishnamurthy, S. M. Spanier

University of Tennessee, Knoxville, Tennessee 37996, USA

R. Eckmann, J. L. Ritchie, A. Satpathy, C. J. Schilling, R. F. Schwitters

University of Texas at Austin, Austin, Texas 78712, USA

J. M. Izen, X. C. Lou, S. Ye

University of Texas at Dallas, Richardson, Texas 75083, USA

F. Bianchi, F. Gallo, D. Gamba

Università di Torino, Dipartimento di Fisica Sperimentale and INFN, I-10125 Torino, Italy

M. Bomben, L. Bosisio, C. Cartaro, F. Cossutti, G. Della Ricca, S. Dittongo, L. Lanceri, L. Vitale

Università di Trieste, Dipartimento di Fisica and INFN, I-34127 Trieste, Italy

V. Azzolini, N. Lopez-March, F. Martinez-Vidal

IFIC, Universitat de Valencia-CSIC, E-46071 Valencia, Spain

Sw. Banerjee, B. Bhuyan, C. M. Brown, D. Fortin, K. Hamano, R. Kowalewski, I. M. Nugent, J. M. Roney,
R. J. Sobie

University of Victoria, Victoria, British Columbia, Canada V8W 3P6

J. J. Back, P. F. Harrison, T. E. Latham, G. B. Mohanty, M. Pappagallo

Department of Physics, University of Warwick, Coventry CV4 7AL, United Kingdom

H. R. Band, X. Chen, B. Cheng, S. Dasu, M. Datta, K. T. Flood, J. J. Hollar, P. E. Kutter, B. Mellado,
A. Mihalyi, Y. Pan, M. Pierini, R. Prepost, S. L. Wu, Z. Yu

University of Wisconsin, Madison, Wisconsin 53706, USA

H. Neal

Yale University, New Haven, Connecticut 06511, USA

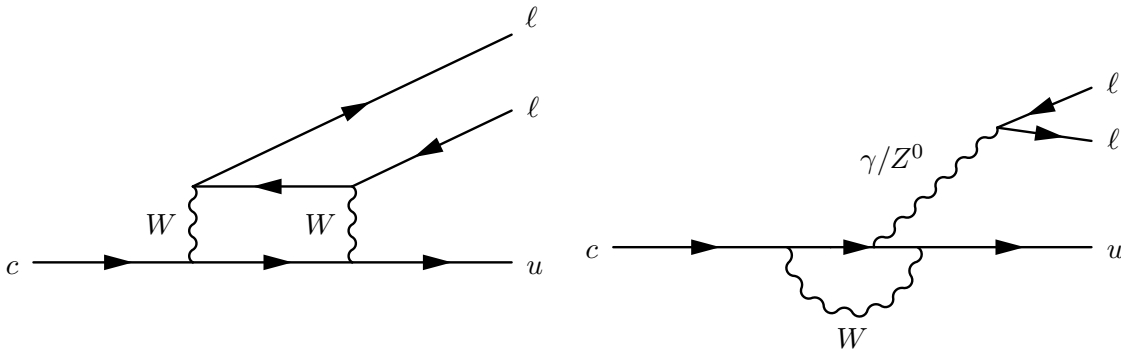


Figure 1: Standard model short-distance contributions to the $c \rightarrow u\ell^+\ell^-$ transition.

1 INTRODUCTION

In the Standard Model (SM), flavor-changing neutral-current (FCNC) processes cannot occur at the tree level. FCNC processes therefore provide an excellent tool for investigating the quantum corrections in the SM as a way to search for evidence of physics beyond the SM. FCNC processes have been studied extensively for K and B mesons in $K^0 - \bar{K}^0$ and $B^0 - \bar{B}^0$ mixing processes and in rare FCNC decays, such as $s \rightarrow d\ell^+\ell^-$, $b \rightarrow s\gamma$ and $b \rightarrow s\ell^+\ell^-$ decays. The present measurements of these processes agree with SM predictions [1], but there are strong ongoing efforts to improve both the measurements and the theoretical predictions, and to measure new effects, such as CP violation, in FCNC processes.

FCNC processes in the charm sector have received less attention and the experimental upper limits are currently above the SM predictions. In the SM very small signals are expected, as a consequence of effective Glashow-Iliopoulos-Maiani (GIM) cancellation. For instance, the $c \rightarrow u\ell^+\ell^-$ transitions illustrated in Fig. 1 lead to branching fractions for $D \rightarrow X_u\ell^+\ell^-$ of $O(10^{-8})$ [2,3]. This contribution is masked by the presence of long-distance contributions from intermediate vector resonances such as $D \rightarrow X_u V, V \rightarrow \ell^+\ell^-$. These are predicted to have branching fractions of $O(10^{-6})$ [2, 3]. In $c \rightarrow u\ell^+\ell^-$ transitions, the effect of these resonances can be separated from short-distance contributions by studying the invariant mass of the $\ell^+\ell^-$ pair. In radiative charm decays, $c \rightarrow u\gamma$, the long-distance contributions make it impossible to study the underlying short-distance physics [4].

Several extensions to the SM have been studied and their impact on $D \rightarrow X_u\ell^+\ell^-$ decay rates estimated [2,5]. The largest possible effect is expected in R-parity violating supersymmetric models. Depending on the size of the R-parity violating couplings, branching fractions of up to $O(10^{-5})$ for different $D \rightarrow X_u\ell^+\ell^-$ decays are possible. This is within the reach of our experimental sensitivity of $O(10^{-6}-10^{-5})$, depending on the decay mode.

There is a large group of possible FCNC charm decays to be measured. The best existing limits are for the branching fractions $\text{BF}(D^0 \rightarrow \ell^+\ell^-)$ [6] and are $O(10^{-6})$ at 90% CL. In this analysis we search for FCNC charm decays of the form $X_c^+ \rightarrow h^+\ell^+\ell^-$, where the two leptons ℓ^+ and ℓ^- can each be either an electron or muon. The charge-conjugate decay modes are implied here and throughout this note. Current upper limits [7–10] range from no limits in some of the baryon modes

Table 1: Branching fractions [11] for the charm decays used for normalization.

Decay mode	Branching Fraction
$D^+ \rightarrow \pi^+\phi$	$(6.2\pm 0.6) \times 10^{-3}$
$D_s^+ \rightarrow \pi^+\phi$	$(36\pm 9) \times 10^{-3}$
$\Lambda_c^+ \rightarrow pK^-\pi^+$	$(50\pm 13) \times 10^{-3}$

to 5×10^{-6} . The FCNC decay combinations we examine are $D^+ \rightarrow \pi^+\ell^+\ell'^-$, $D_s^+ \rightarrow K^+\ell^+\ell'^-$ and $\Lambda_c^+ \rightarrow p\ell^+\ell'^-$. Decays where the two leptons are of different flavor are lepton-family violating and therefore forbidden in the SM. We also search for $D^+ \rightarrow K^+\ell^+\ell'^-$ and $D_s^+ \rightarrow \pi^+\ell^+\ell'^-$ decays, but these require both quarks in the charm meson to change flavor.

The only long-distance contributions relevant at the current experimental sensitivity are from $D^+ \rightarrow \pi^+\phi$ and $D_s^+ \rightarrow \pi^+\phi$ decays. The branching fractions to $\pi^+\ell^+\ell^-$ through these two resonance decays are 1.8×10^{-6} and 1.1×10^{-5} , respectively [11]. In this analysis, we measure the total rate of decay excluding a region around the ϕ resonance in the invariant mass of the $\ell^+\ell^-$ pair.

The measured FCNC decay yields are converted into branching ratios by normalizing them to the yields of known charm decays. We choose normalization modes that have kinematics similar to the FCNC decays, so that most of the systematic effects not related to particle identification cancel in the branching ratio. For the D^+ and D_s^+ decays we use decays to $\pi^+\phi$ and for the Λ_c^+ we use $\Lambda_c^+ \rightarrow pK^-\pi^+$ decays. The measured branching fractions for these modes are listed in Table 1. The ϕ decays are reconstructed in only the K^+K^- decay modes. This introduces an additional branching fraction for $\phi \rightarrow K^+K^-$, which is 0.491 ± 0.006 [11]. We use the abbreviation $D_{(s)}^+ \rightarrow \pi^+\phi_{KK}$ to denote the $D_{(s)}^+ \rightarrow \pi^+\phi$, $\phi \rightarrow K^+K^-$ decays.

2 THE BABAR DETECTOR AND DATASET

The measurements are performed using data collected by the BABAR detector [12] at the PEP-II storage ring at SLAC. The data sample used comprises an integrated luminosity of 263 fb^{-1} collected from e^+e^- collisions at the $\Upsilon(4S)$ resonance and 25 fb^{-1} collected 40 MeV below the $\Upsilon(4S)$ resonance. For event simulation we use the Monte Carlo (MC) generator EVTGEN [13] with a full detector simulation based on GEANT4 [14]. Signal and the $\Lambda_c^+ \rightarrow pK^-\pi^+$ MC events are generated with a 3-body phase-space distribution while $D_{(s)}^+ \rightarrow \pi^+\phi_{KK}$ MC events are generated with a Breit-Wigner for the ϕ decay. All signal events are simulated as $c\bar{c}$ continuum events. Samples of simulated generic $c\bar{c}$ and uds continuum events and $B\bar{B}$ decays corresponding to 1.4–5 times the recorded data sample are used to study background contributions.

3 ANALYSIS METHOD

Initial charm hadron candidates are formed from one track identified as either a pion, kaon or proton and two tracks each of which is identified as an electron or a muon. Typical electron (muon) identification efficiency is about 94% (60%). Hadron identification efficiencies average about 98%, 87% and 80% for pions, kaons and protons, respectively. The two tracks identified as leptons are required to have opposite charge. For candidates with a pion or kaon track, the

invariant mass of the charm candidate is required to be between 1.7 and 2.1 GeV/ c^2 , while for the candidates with protons it is required to be between 2.2 and 2.4 GeV/ c^2 . Charm hadrons from continuum production typically carry most of the energy of the initial quarks. We therefore require the momentum, p^* , of the charm hadron candidate in the e^+e^- center-of-mass frame to be larger than 2.8 to 3.5 GeV/ c depending on decay mode. This removes a large fraction of the background. Charm hadrons produced in B decays are kinematically limited to be below about 2.2 GeV/ c and are therefore not used in this analysis.

After the initial event selection, significant combinatoric background contributions remain from semileptonic B decays and low-multiplicity QED events. These background sources have been studied using events from invariant mass sidebands in data and from MC samples. The final event selection criteria are chosen based on these studies to minimize the expected upper limit on the $X_c^+ \rightarrow h^+\ell^+\ell'^-$ branching ratio under the assumption that no signal is present.

The QED events are mainly radiative Bhabha, initial state radiation and two-photon events. These are easily identified by their low multiplicity and/or highly jet-like structure. They are suppressed by requiring at least five tracks in an event and a minimum event sphericity [15] of 0.13 calculated in the e^+e^- center-of-mass frame.

We suppress the background from semileptonic B decays by rejecting events with evidence of neutrinos and requiring the two leptons to come from a common point. The latter is achieved by a tight requirement on the probability of the vertex fit χ^2 ($P(\chi^2) > 0.05$) and on the distance of closest approach between the two leptons ($< 250 \mu\text{m}$).

The neutrinos are not directly detected and therefore show up as missing energy in the event. This is measured in two ways. We first calculate the total energy in an event from all reconstructed neutral clusters and tracks in an event, assuming the pion mass for tracks. Second we calculate the net transverse momentum in an event (with respect to the beam axis) by adding the momentum vectors of all neutral clusters and tracks. The neutral clusters are assumed to be photons. The more the transverse momentum deviates from zero the more likely it is to be a semileptonic B decay. Figure 2 shows the distributions of the two variables for $D^+ \rightarrow \pi^+e^+e^-$ signal MC events and for $\pi^+e^+e^-$ candidates in generic MC B^+B^- events. Selecting on a linear combination of the two variables as indicated in the figure, 74% of the signal events are kept while 84% of the B^+B^- events are rejected.

In the e^+e^- decay modes, there is a significant contribution at low e^+e^- mass from π^0 decays. Some of these are from decays directly to $e^+e^-(\gamma)$ while others are $\pi^0 \rightarrow \gamma\gamma$, where one of the photons converts to e^+e^- . These are removed together with γ conversions by requiring $m(e^+e^-) > 200 \text{ MeV}/c^2$.

For $D_s^+ \rightarrow \pi^+\ell^+\ell'^-$ decays, we furthermore require the presence of a photon candidate with an energy above 100 MeV and $|m(h\ell^+\ell'^-\gamma) - m(h\ell^+\ell'^-) - 0.1438 \text{ MeV}/c^2| < 0.015 \text{ MeV}/c^2$. This selects D_s^+ mesons coming from $D_s^{*+} \rightarrow D_s^+\gamma$ decays and helps reduce the non- D_s^+ background.

The requirement on the momentum p^* of the charm hadron is decay mode dependent:

- For $D^+ \rightarrow h\ell^+\ell'^-$, $p^* > 3.3 \text{ GeV}/c$.
- For $D_s^+ \rightarrow h\ell^+\ell'^-$, $p^* > 3.5 \text{ GeV}/c$.
- For $\Lambda_c^+ \rightarrow p\ell^+\ell'^-$, $p^* > 2.8 \text{ GeV}/c$.

For the $D_{(s)}^+ \rightarrow \pi^+\ell^+\ell'^-$ decay modes, we exclude events with $0.95 < m(e^+e^-) < 1.05 \text{ GeV}/c^2$ and $0.99 < m(\mu^+\mu^-) < 1.05 \text{ GeV}/c^2$. The excluded regions for the two decay modes are different

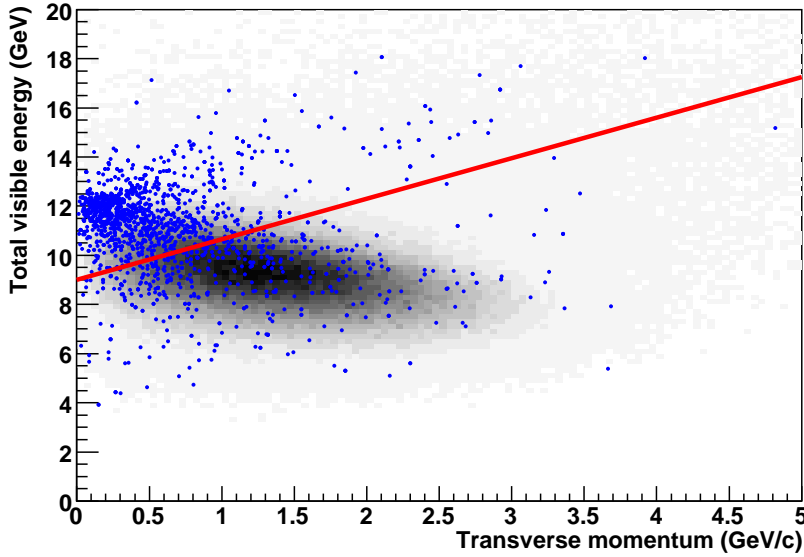


Figure 2: Total energy vs net transverse momentum for $D^+ \rightarrow \pi^+ e^+ e^-$ MC signal events (points) and background events from generic $B^+ B^-$ events (shaded histogram) for the $\pi^+ e^+ e^-$ mode. The events below the red line are rejected in the final event selection.

due to the larger radiative tails in the $\pi^+ e^+ e^-$ decay mode. In order to make further cross-checks, we also select a sample with $D_{(s)}^+ \rightarrow \pi^+ \phi, \phi \rightarrow \ell^+ \ell^-$ candidates. For this sample we require $0.995 \text{ GeV}/c^2 < m(e^+ e^-) < 1.030 \text{ GeV}/c^2$, $1.005 \text{ GeV}/c^2 < m(\mu^+ \mu^-) < 1.030 \text{ GeV}/c^2$ and $p^* > 3.1 \text{ GeV}/c$.

For the normalization decay modes the same selection is applied except for the lepton particle identification requirements and the restriction on the distance of closest approach between the two lepton candidates. Instead the kaons and pions in the $D_{(s)}^+ \rightarrow \pi^+ \phi_{KK}$ and $\Lambda_c^+ \rightarrow p K^- \pi^+$ decay modes are required to be specifically identified. For the $D_{(s)}^+ \rightarrow \pi^+ \phi_{KK}$ decay modes, we further require the invariant mass of the kaon pair to be within $15 \text{ MeV}/c^2$ of the world-average value for the ϕ mass [11]. Since the selection of $D_s^+ \rightarrow \pi^+ \ell^+ \ell^-$ decays requires the presence of a photon from $D_s^{*+} \rightarrow D_s^+ \gamma$ decays whereas the $D_s^+ \rightarrow K^+ \ell^+ \ell^-$ selection does not, the selection of $D_s^+ \rightarrow \pi^+ \phi_{KK}$ decays is performed separately for the two decay modes.

The invariant mass distributions of the $h^+ \ell^+ \ell^-$ candidates are fitted using an extended unbinned maximum likelihood fit. The probability density function (PDF) for signal events is given by the so-called Crystal Ball function [16] in order to account for radiative tails:

$$P_{CB}(m; \mu, \sigma, \alpha, n) = \begin{cases} e^{-0.5(\frac{m-\mu}{\sigma})^2} & \text{if } m \geq \mu - \alpha\sigma. \\ e^{-0.5\alpha^2 \left(\frac{n\sigma}{n\sigma - \alpha^2\sigma - \alpha(m-\mu)} \right)^n} & \text{if } m < \mu - \alpha\sigma. \end{cases} \quad (1)$$

The four parameters, μ, σ, α and n , are obtained from fits to signal MC and kept fixed during fits to the data, leaving only the overall normalization as a free parameter. The fitted width of the Gaussian component (σ) is found to lie between 6 and $9 \text{ MeV}/c^2$ depending on the decay mode. The MC events have been corrected to reproduce particle identification efficiencies measured in various control modes. The yields from the MC fits are used to calculate the signal efficiencies,

which range between 0.3 and 5.3%. The modes with low efficiency are decays with two muons and decays requiring a photon from D_s^{*+} decays. The muon identification efficiency is very low for muons with momentum below $1 \text{ GeV}/c$.

For the normalization decay modes, the radiative effects are negligible and we use the sum of two Gaussian distributions with a common mean to describe the D^+ , D_s^+ and A_c^+ signals. All parameters are free in the fits to data.

The invariant mass distribution of the combinatoric background events for the signal modes are described by first-order polynomials. For the normalization decay modes, a second-order polynomial is used. The background parameters are allowed to vary freely in all cases.

An additional background comes from hadronic charm decays where two hadrons are misidentified as leptons. Pions have a probability of about 2% (0.1%) to be identified as a muon (electron) depending on the pion momentum and angle. This background component is negligible in the signal modes with electrons and is therefore only included in decay modes with two muons. The shape of this background is obtained from MC samples of hadronic three-body charm decays. Each event is weighted according to the probability of misidentifying a pion as a muon. The misidentification probability is measured from data using samples of $D^0 \rightarrow K^- \pi^+$ decays. The misidentified hadronic charm decays are reconstructed at slightly lower $h^+ \mu^+ \mu^-$ mass than the signal events. The peak mass is shifted by about $15 \text{ MeV}/c^2$ which is sufficient separation for the yield to be determined by the likelihood fit instead of relying on the MC prediction.

For the charm meson modes two signals are fitted simultaneously since the D^+ and D_s^+ mesons can decay to the same final state. However, since the optimal event selection criteria are different for the D^+ and D_s^+ modes, only one of the fitted yields is used from each fit.

For most modes we do not see a significant signal; in addition to determining a central value for the yields, we set upper limits on the branching ratios at 90% confidence level (CL). This is chosen as the point where the negative log likelihood is 1.355 above its minimum value. In order to always have a physical (positive) upper limit, we only consider the minimum at or above 0 signal events. This generally results in conservative confidence intervals. Systematic uncertainties from the signal efficiency and the normalization mode, detailed in the next section, are included as a Gaussian constraint in the likelihood expression.

4 SYSTEMATIC STUDIES

Most systematic effects are expected to cancel in the branching ratio since they affect the signal and normalization modes equally. We therefore only have to account for differences in selection, acceptance and decay kinematics. Table 2 gives a summary of all the systematic uncertainties related to the branching ratio calculation. An additional systematic is assigned for the estimation of the signal yield. The details of the different uncertainties are given below.

Systematic uncertainties related to the signal PDF parameters obtained from MC are investigated in two ways. First, the PDF parameters for data and MC are compared in the fits to the normalization modes. Differences can be due either to general data-MC tracking differences or to uncertainty in the PDG mass used in the simulation. Second, fits to the invariant mass of $J/\psi \rightarrow \ell^+ \ell^-$ candidates from inclusive B decays are compared between data and MC. The second comparison is sensitive to effects associated with lepton reconstruction. Based on these studies, fits with the mean mass shifted by up to $2.5 \text{ MeV}/c^2$, depending on the decay mode, are performed. Based on the same studies, the widths of the signal PDFs are changed by $\pm 3\%$. The fit giving the highest upper limit on the branching ratio is used for the final result.

Table 2: Summary of the multiplicative systematic uncertainties for all the decay modes. DOCA is the uncertainty due to the distance of closest approach requirement and PID is the uncertainty from the particle identification.

Decay mode	Normalization					
	Mode	MC stat.	DOCA	PID	p^*	Total
$D^+ \rightarrow \pi^+ e^+ e^-$	3.7%	1.0%	0.3%	3%	2%	5.3%
$D^+ \rightarrow \pi^+ \mu^+ \mu^-$	3.7%	1.8%	0.3%	5%	2%	6.8%
$D^+ \rightarrow \pi^+ e^+ \mu^-$	3.7%	1.3%	0.3%	3%	2%	5.3%
$D^+ \rightarrow \pi^+ \mu^+ e^-$	3.7%	1.3%	0.3%	3%	2%	5.3%
$D_s^+ \rightarrow \pi^+ e^+ e^-$	4.0%	1.8%	0.3%	3%	2%	5.7%
$D_s^+ \rightarrow \pi^+ \mu^+ \mu^-$	4.0%	3.3%	0.3%	5%	2%	7.5%
$D_s^+ \rightarrow \pi^+ e^+ \mu^-$	4.0%	2.3%	0.3%	3%	2%	5.9%
$D_s^+ \rightarrow \pi^+ \mu^+ e^-$	4.0%	2.3%	0.3%	3%	2%	5.9%
$D^+ \rightarrow K^+ e^+ e^-$	3.7%	1.1%	0.3%	4%	2%	5.9%
$D^+ \rightarrow K^+ \mu^+ \mu^-$	3.7%	2.2%	0.3%	5%	2%	6.9%
$D^+ \rightarrow K^+ e^+ \mu^-$	3.7%	1.5%	0.3%	4%	2%	6.0%
$D^+ \rightarrow K^+ \mu^+ e^-$	3.7%	1.5%	0.3%	4%	2%	6.0%
$D_s^+ \rightarrow K^+ e^+ e^-$	3.7%	1.1%	0.3%	4%	2%	5.9%
$D_s^+ \rightarrow K^+ \mu^+ \mu^-$	3.7%	2.3%	0.3%	5%	2%	6.9%
$D_s^+ \rightarrow K^+ e^+ \mu^-$	3.7%	1.6%	0.3%	4%	2%	6.0%
$D_s^+ \rightarrow K^+ \mu^+ e^-$	3.7%	1.6%	0.3%	5%	2%	6.7%
$\Lambda_c^+ \rightarrow p e^+ e^-$	2.5%	1.0%	0.3%	2%	2%	3.9%
$\Lambda_c^+ \rightarrow p \mu^+ \mu^-$	2.5%	2.3%	0.3%	4%	2%	5.6%
$\Lambda_c^+ \rightarrow p e^+ \mu^-$	2.5%	1.7%	0.3%	3%	2%	4.7%
$\Lambda_c^+ \rightarrow p \mu^+ e^-$	2.5%	1.7%	0.3%	3%	2%	4.7%
$D^+ \rightarrow \pi^+ \phi_{e^+ e^-}$	3.7%	0.8%	0.3%	3%	2%	5.2%
$D^+ \rightarrow \pi^+ \phi_{\mu^+ \mu^-}$	3.7%	1.7%	0.3%	5%	2%	6.8%
$D_s^+ \rightarrow \pi^+ \phi_{e^+ e^-}$	3.7%	0.8%	0.3%	3%	2%	5.2%
$D_s^+ \rightarrow \pi^+ \phi_{\mu^+ \mu^-}$	3.7%	1.6%	0.3%	5%	2%	6.7%

For the background shape assumption, the signal fits are repeated using a second order polynomial as the background PDF instead of the nominal first order polynomial. The result of the fit with the higher limit is used to quote the upper limit, unless variations of the signal PDF yield an even higher limit.

In the normalization modes, the statistical uncertainties from the fits, the MC statistics and uncertainties from the signal and background shapes are all at or below 1%. The main uncertainty related to the normalization modes comes from how the efficiency is affected by sub-resonances in the decays. This is estimated to be about 3.5% for each of the $D_{(s)}^+$ modes and 1.1% for the $\Lambda_c^+ \rightarrow pK^-\pi^+$ mode.

The requirement that the distance of closest approach between the two leptons be below $250 \mu\text{m}$ is not applied to the normalization mode and any MC-data difference can therefore not be expected to cancel in the branching ratio. Studies of the $J/\psi \rightarrow \ell^+\ell^-$ samples show efficiency differences between data and MC to be less than 0.3%.

The efficiency of the particle identification has associated systematic uncertainties. We assign 0.6% for each pion, 1.1% for each kaon, 1% for each electron and 2% for each muon. We do not apply a systematic uncertainty for the protons, since both the signal and the normalization mode contain a proton and the uncertainty therefore cancels. Uncertainties from the same types of particles are added linearly, while for different types they are added in quadrature.

The efficiencies of the signal and normalization modes do not have the same dependence on p^* . Varying the p^* distribution used in the MC to better match the data changes the ratio of signal and normalization mode efficiencies by less than 2% for all decay modes.

In the calculation of the signal efficiency we assume that the decays follow a three-body phase-space model. The selection efficiency has some dependence on where the decay lies in the Dalitz plane, so this assumption introduces a systematic uncertainty. Ignoring the regions we explicitly remove in the selection and the very high end of the $m(\ell^+\ell^-)$ distribution, the efficiency typically varies less than 25% around the average as a function of $m(\ell^+\ell^-)$. This model dependence is not included in the systematic uncertainty.

5 PHYSICS RESULTS

The invariant mass distributions of the normalization decay modes and the corresponding fits are shown in Fig. 3. The $\pi^+K^+K^-$ invariant mass distribution has both D^+ and D_s^+ signals and is shown multiple times, because the D^+ and D_s^+ selections have different p^* requirements and the $D_s^+ \rightarrow \pi^+\ell^+\ell^-$ selection requires a γ from a D_s^{*+} decay. Each selection requires its own fit in order to cancel most systematic uncertainties. The fitted signal yields are listed in Table 3. The table also lists the efficiencies estimated from signal MC.

The invariant mass distributions for signal candidates in all 20 decay modes are shown in Figs. 4–8. The yields obtained from unbinned likelihood fits are listed in Table 4 with statistical and systematic uncertainties. Only systematic uncertainties associated with the signal and background PDFs are included in the systematic uncertainty for the yields. The curves representing the fits are overlaid in the figures. No significant signals are seen and we calculate upper limits on the branching ratios $\frac{\Gamma(D_{(s)}^+ \rightarrow \pi^+\ell^+\ell^-)}{\Gamma(D_{(s)}^+ \rightarrow \pi^+\phi)}$, $\frac{\Gamma(D_{(s)}^+ \rightarrow K^+\ell^+\ell^-)}{\Gamma(D_{(s)}^+ \rightarrow \pi^+\phi)}$ and $\frac{\Gamma(\Lambda_c^+ \rightarrow p\ell^+\ell^-)}{\Gamma(\Lambda_c^+ \rightarrow pK^-\pi^+)}$ at 90% CL. For comparison with previous measurements, the upper limits on the total branching fraction (BF) at 90% CL, calculated using Table 1, are also given.

The background from misidentified $D_s^+ \rightarrow \pi^+\pi^+\pi^-$ decays in the $D_s^+ \rightarrow \pi^+\mu^+\mu^-$ decay channel

Table 3: MC efficiency and fitted yields in data for the normalization modes. The $\pi^+K^+K^-$ distribution is fitted after the different selection criteria matching those for the corresponding signal modes are applied.

Decay mode	Selection Mode	N_{sig}	Efficiency
$D^+ \rightarrow \pi^+ \phi_{KK}$	$D^+ \rightarrow \pi^+ / K^+ \ell^+ \ell'^-$	25825 ± 200	$(4.77 \pm 0.04)\%$
$D_s^+ \rightarrow \pi^+ \phi_{KK}$	$D_s^+ \rightarrow \pi^+ \ell^+ \ell'^-$	23372 ± 162	$(1.26 \pm 0.02)\%$
$D_s^+ \rightarrow \pi^+ \phi_{KK}$	$D_s^+ \rightarrow K^+ \ell^+ \ell'^-$	71501 ± 307	$(3.77 \pm 0.04)\%$
$\Lambda_c^+ \rightarrow p K^- \pi^+$	$\Lambda_c^+ \rightarrow p \ell^+ \ell'^-$	212664 ± 1028	$(7.38 \pm 0.07)\%$
$D^+ \rightarrow \pi^+ \phi_{KK}$	$D^+ \rightarrow \pi^+ \phi_{\ell^+ \ell^-}$	32920 ± 329	$(6.12 \pm 0.05)\%$
$D_s^+ \rightarrow \pi^+ \phi_{KK}$	$D_s^+ \rightarrow \pi^+ \phi_{\ell^+ \ell^-}$	115480 ± 413	$(6.49 \pm 0.05)\%$

is found to be 5 ± 2 times larger than expected from the weighted MC, while in all other muon modes no significant component of this background is visible. Cross checks of the MC did not lead to an explanation for the high level of this background in the $D_s^+ \rightarrow \pi^+ \mu^+ \mu^-$ decay channel. Fitting the $\pi^+ \mu^+ \mu^-$ candidate mass distribution with the misidentification component fixed to 0 gives a signal yield of 0.2 events with little change in the upper limit.

Figure 9 summarizes the previously published and the new limits. For most decay modes, this analysis gives a significant improvement over the existing measurements. A recent CLEO measurement [7] is slightly more sensitive to $D^+ \rightarrow \pi^+ e^+ e^-$ decays, and our sensitivity to $D^+ \rightarrow \pi^+ \mu^+ \mu^-$ and $D^+ \rightarrow K^+ \mu^+ \mu^-$ decays is worse than fixed target experiments [9] due to the low muon efficiency and high backgrounds. The D0 collaboration has recently presented a preliminary result [8] that improves the limit on $D^+ \rightarrow \pi^+ \mu^+ \mu^-$ decays to 4.7×10^{-6} .

The $D_{(s)}^+ \rightarrow \pi^+ \phi_{e^+ e^-}$ and $D_{(s)}^+ \rightarrow \pi^+ \phi_{\mu^+ \mu^-}$ candidates are shown in Fig. 10. Signals are seen for all decays except for $D^+ \rightarrow \pi^+ \phi_{\mu^+ \mu^-}$. Table 5 gives the fit yields and $\phi \rightarrow \ell^+ \ell^-$ branching fractions calculated by normalizing to the $D_{(s)}^+ \rightarrow \pi^+ \phi_{KK}$ decay modes. The significance is calculated from the change in likelihood with and without any signal. The observed branching fractions are in agreement with the world averages [11] of $(2.98 \pm 0.04) \times 10^{-4}$ for $\phi \rightarrow e^+ e^-$ and $(2.85 \pm 0.19) \times 10^{-4}$ for $\phi \rightarrow \mu^+ \mu^-$.

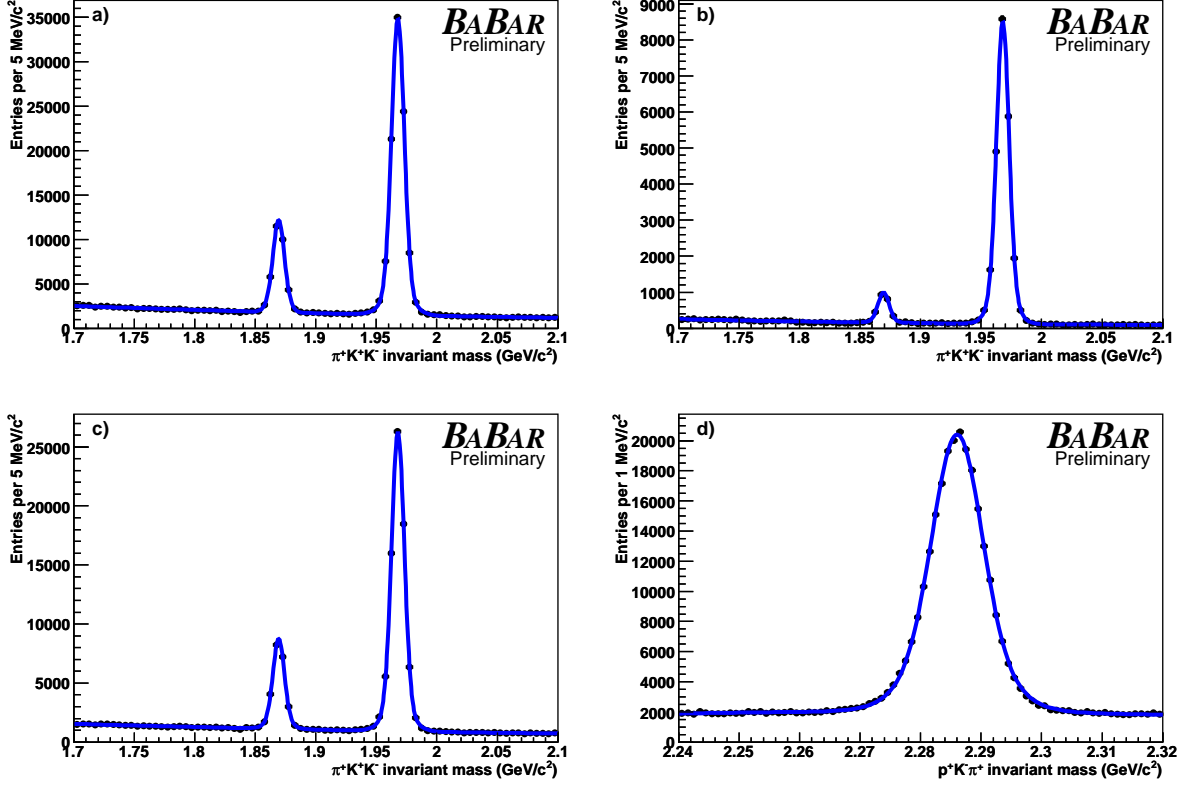


Figure 3: Invariant mass distribution for $\pi^+\phi_{K+K^-}$ candidates with a) $D^+ \rightarrow \pi^+\ell^+\ell'^-$ and $D^+ \rightarrow K^+\ell^+\ell'^-$ selection criteria, b) $D_s^+ \rightarrow \pi^+\ell^+\ell'^-$ selection criteria and c) $D_s^+ \rightarrow K^+\ell^+\ell'^-$ selection criteria. d) Invariant mass distribution for $\Lambda_c^+ \rightarrow pK^-\pi^+$ candidates with the $\Lambda_c^+ \rightarrow p\ell^+\ell'^-$ selection criteria. The solid lines are the result of a fit to double-Gaussian signals and a second-order polynomial for the background.

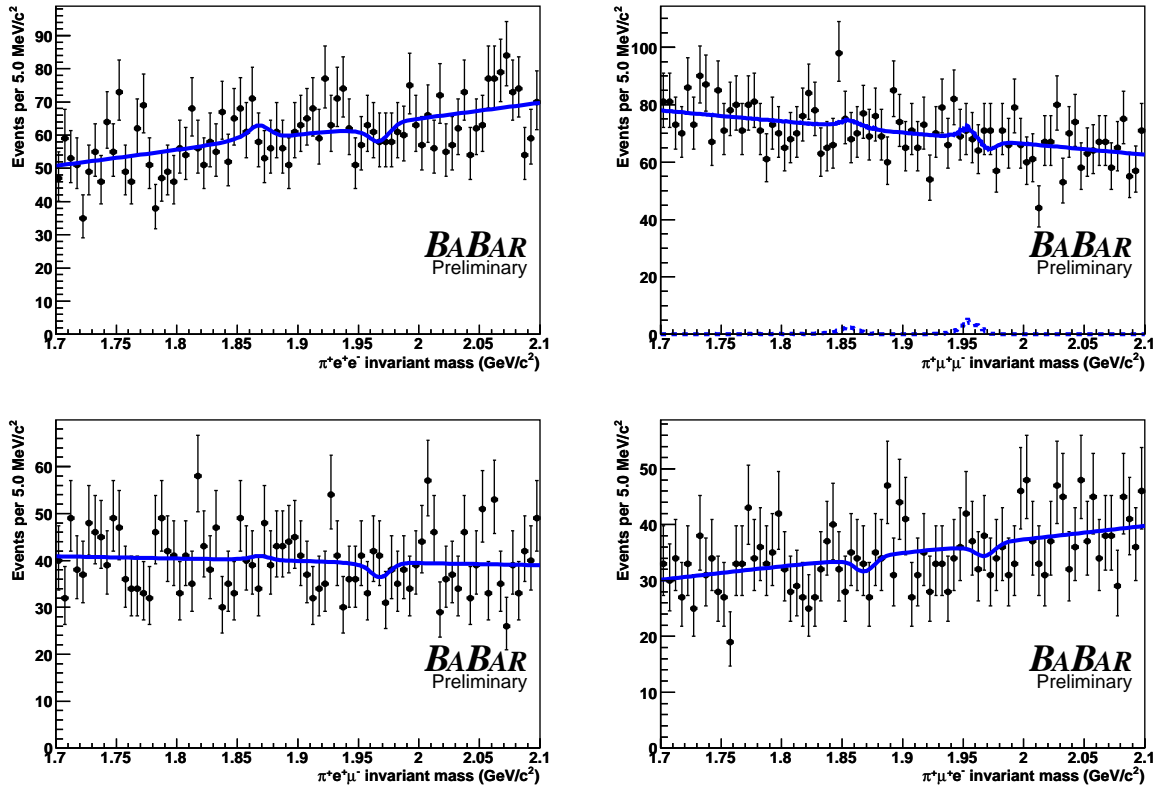


Figure 4: Invariant mass distribution for $D^+ \rightarrow \pi^+ \ell^+ \ell'^-$ candidates. The solid lines are the results of the fits. The misidentified background component in the dimuon mode is shown as a dashed curve.

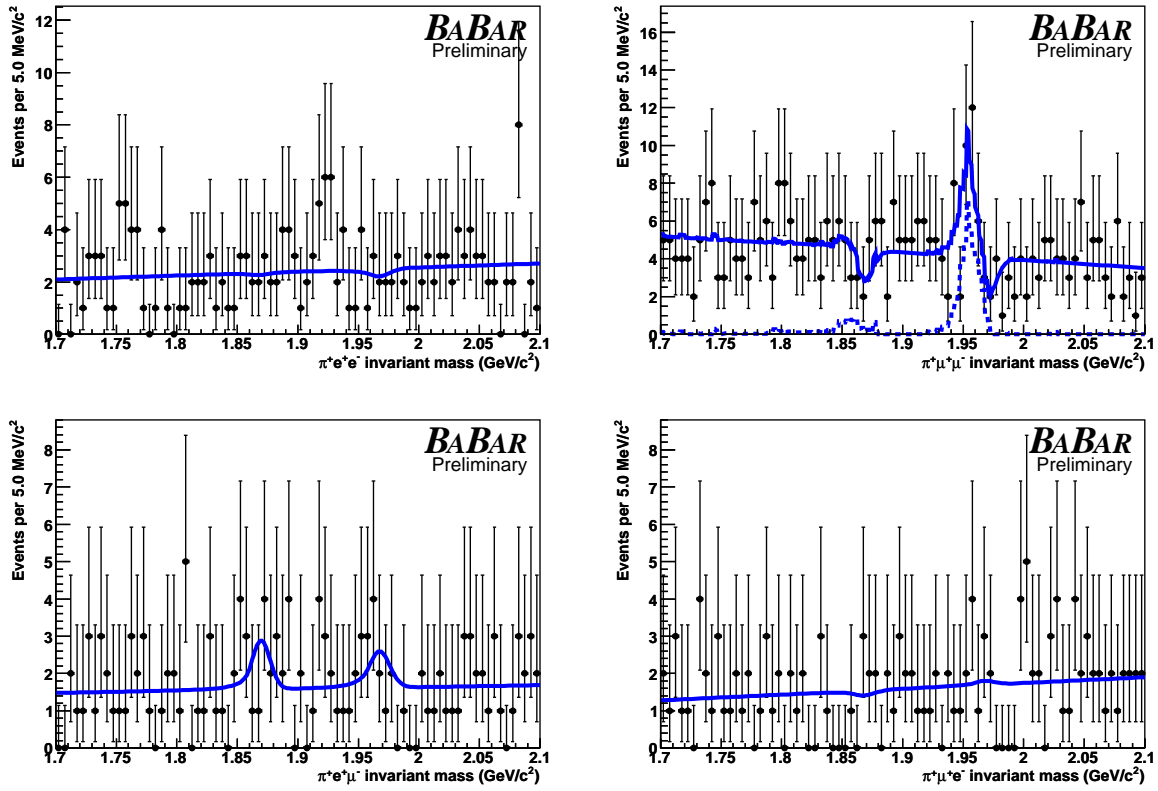


Figure 5: Invariant mass distribution for $D_s^+ \rightarrow \pi^+ \ell^+ \ell'^-$ candidates. The solid lines are the results of the fits. The misidentified background component in the dimuon mode is shown as a dashed curve.

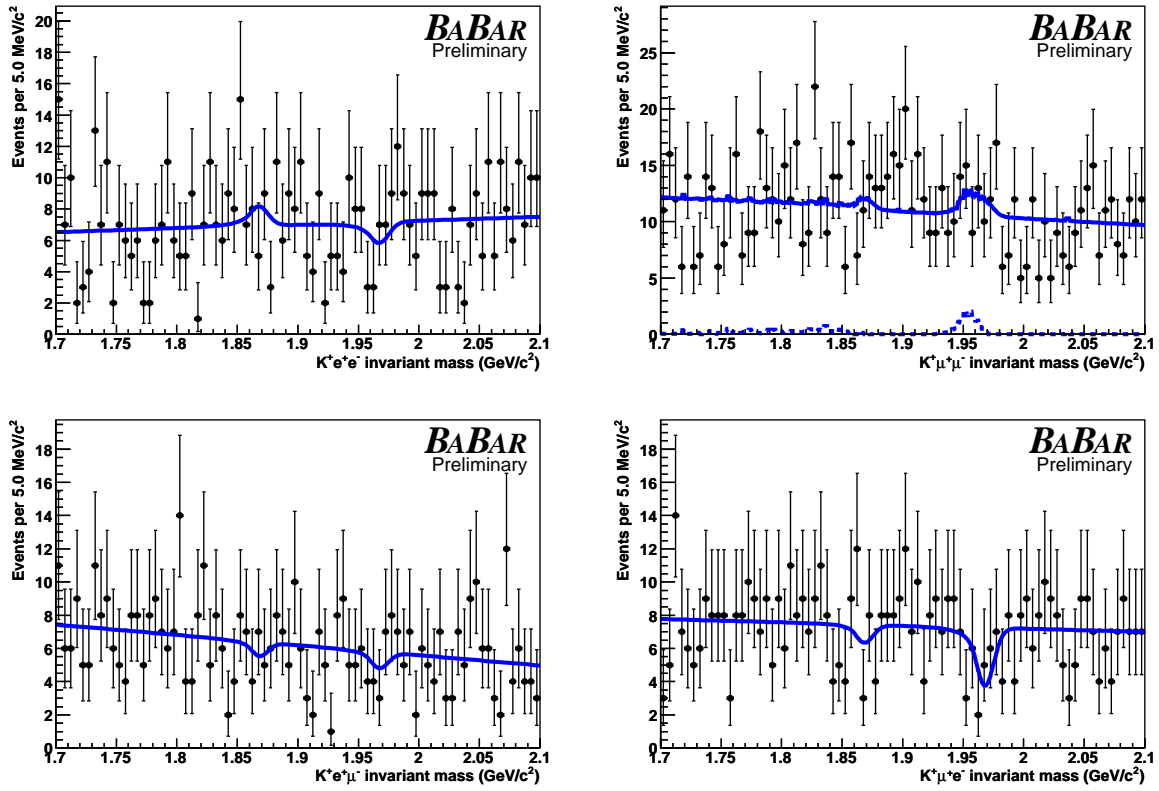


Figure 6: Invariant mass distribution for $D^+ \rightarrow K^+ \ell^+ \ell'^-$ candidates. The solid lines are the results of the fits. The misidentified background component in the dimuon mode is shown as a dashed curve.

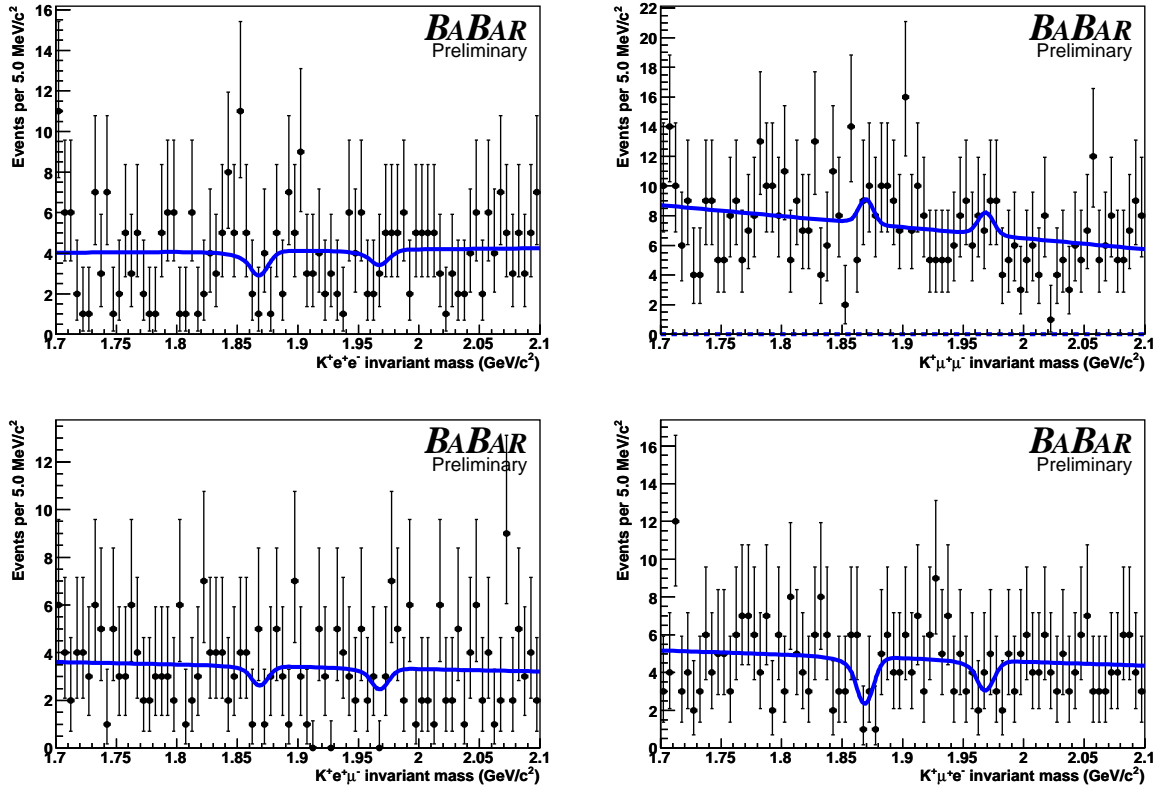


Figure 7: Invariant mass distribution for $D_s^+ \rightarrow K^+ \ell^+ \ell'^-$ candidates. The solid lines are the results of the fits. The misidentified background component in the dimuon mode is shown as a dashed curve.

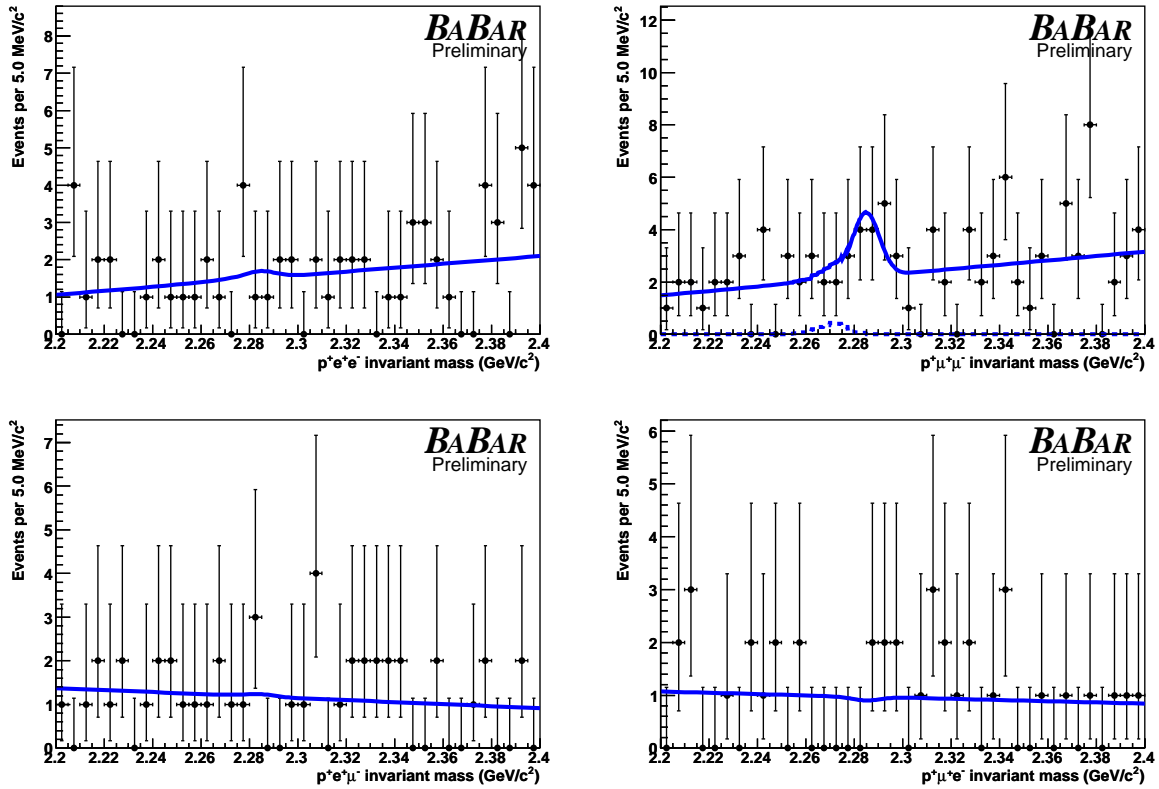


Figure 8: Invariant mass distribution for $\Lambda_c^+ \rightarrow p \ell^+ \ell'^-$ candidates. The solid lines are the results of the fits. The misidentified background component in the dimuon mode is shown as a dashed curve.

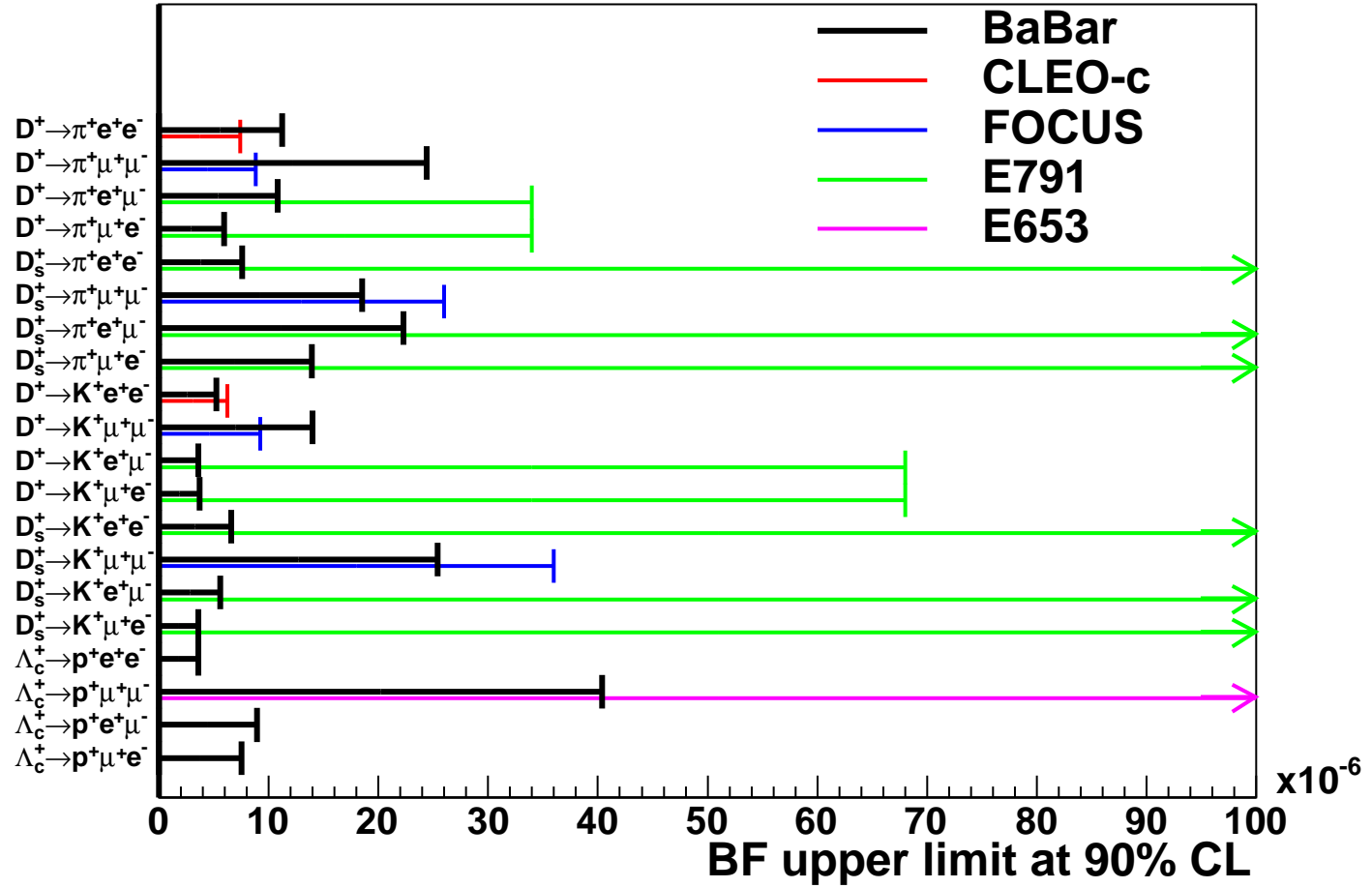


Figure 9: Comparison of the branching fraction limits measured in this note with previously published measurements [7,9,10].

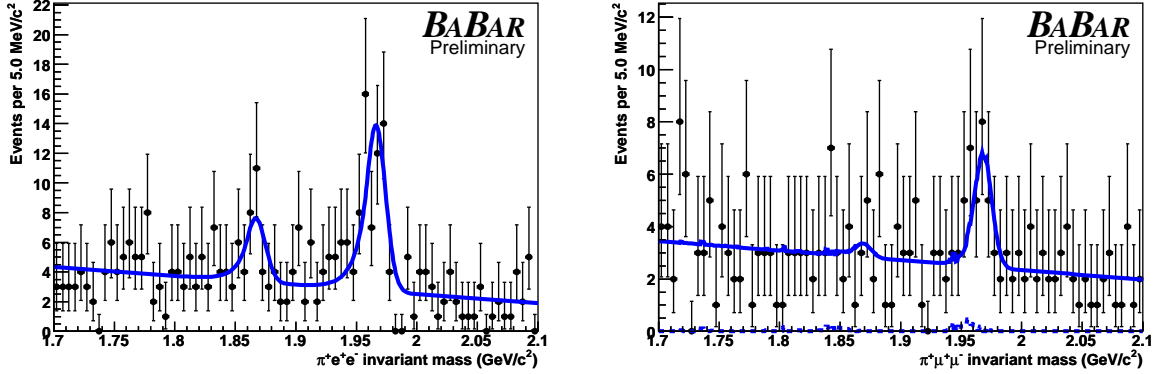


Figure 10: Invariant mass distribution for (left) $D_{(s)}^+ \rightarrow \pi^+ \phi_{e^+e^-}$ and (right) $D_{(s)}^+ \rightarrow \pi^+ \phi_{\mu^+\mu^-}$ candidates. The solid lines are the results of the fits. The misidentified background component in the dimuon mode is shown as a dashed curve.

6 SUMMARY

A search for the decay modes $D_{(s)}^+ \rightarrow \pi^+ \ell^+ \ell'^-$, $D_{(s)}^+ \rightarrow K^+ \ell^+ \ell'^-$ and $\Lambda_c^+ \rightarrow p \ell^+ \ell'^-$ has been performed using 288 fb^{-1} of e^+e^- data. No signals are observed and we obtain upper limits on the branching ratios $\frac{\Gamma(D_{(s)}^+ \rightarrow \pi^+ \ell^+ \ell'^-)}{\Gamma(D_{(s)}^+ \rightarrow \pi^+ \phi)}$, $\frac{\Gamma(D_{(s)}^+ \rightarrow K^+ \ell^+ \ell'^-)}{\Gamma(D_{(s)}^+ \rightarrow \pi^+ \phi)}$ and $\frac{\Gamma(\Lambda_c^+ \rightarrow p \ell^+ \ell'^-)}{\Gamma(\Lambda_c^+ \rightarrow p K^- \pi^+)}$ between 10^{-4} and 40×10^{-4} at 90% CL. This corresponds to limits on the branching fractions between 4×10^{-6} and 4×10^{-5} . These limits are calculated under the assumption of three-body phase-space decays; the efficiency varies by up to 25% as a function of dilepton invariant mass. For 17 out of the 20 decay modes, the limits are an improvement over the existing measurements.

7 ACKNOWLEDGMENTS

We are grateful for the extraordinary contributions of our PEP-II colleagues in achieving the excellent luminosity and machine conditions that have made this work possible. The success of this project also relies critically on the expertise and dedication of the computing organizations that support BABAR. The collaborating institutions wish to thank SLAC for its support and the kind hospitality extended to them. This work is supported by the US Department of Energy and National Science Foundation, the Natural Sciences and Engineering Research Council (Canada), Institute of High Energy Physics (China), the Commissariat à l'Énergie Atomique and Institut National de Physique Nucléaire et de Physique des Particules (France), the Bundesministerium für Bildung und Forschung and Deutsche Forschungsgemeinschaft (Germany), the Istituto Nazionale di Fisica Nucleare (Italy), the Foundation for Fundamental Research on Matter (The Netherlands), the Research Council of Norway, the Ministry of Science and Technology of the Russian Federation, and the Particle Physics and Astronomy Research Council (United Kingdom). Individuals have received support from the Marie-Curie IEF program (European Union) and the A. P. Sloan Foundation.

Table 4: Yields from fits to the candidates in the 20 $X_c^+ \rightarrow h^+ \ell^+ \ell'^-$ decay modes. The first error is statistical and the second the systematic error on the yield. The third column shows the estimated signal efficiency. The fourth column shows the 90% CL upper limits on the branching ratios of the signal mode to the normalization mode. The last column shows the limits on the branching fraction for the signal modes at 90% CL. The upper limits include all systematic uncertainties.

Decay mode	Yield (events)	Efficiency	BR (10^{-4}) (90% CL)	BF (10^{-6}) (90% CL)
$D^+ \rightarrow \pi^+ e^+ e^-$	$24.0^{+25.0+3.4}_{-24.1-5.1}$	3.93%	< 17.7	< 11.2
$D^+ \rightarrow \pi^+ \mu^+ \mu^-$	$1.5^{+20.1+3.4}_{-19.3-2.6}$	1.09%	< 38.7	< 24.4
$D^+ \rightarrow \pi^+ e^+ \mu^-$	$4.1^{+17.8+3.1}_{-16.3-2.1}$	2.27%	< 17.1	< 10.8
$D^+ \rightarrow \pi^+ \mu^+ e^-$	$-12.1^{+15.5+3.2}_{-14.8-0.0}$	2.29%	< 9.3	< 5.9
$D_s^+ \rightarrow \pi^+ e^+ e^-$	$-1.7^{+5.3+0.2}_{-4.6-2.0}$	1.14%	< 2.1	< 7.6
$D_s^+ \rightarrow \pi^+ \mu^+ \mu^-$	$-9.4^{+5.0+0.2}_{-4.4-1.4}$	0.31%	< 5.1	< 18.5
$D_s^+ \rightarrow \pi^+ e^+ \mu^-$	$4.8^{+4.7+0.8}_{-3.9-0.3}$	0.66%	< 6.2	< 22.3
$D_s^+ \rightarrow \pi^+ \mu^+ e^-$	$0.5^{+4.0+1.0}_{-3.3-0.1}$	0.65%	< 3.8	< 13.9
$D^+ \rightarrow K^+ e^+ e^-$	$5.9^{+8.9+3.8}_{-7.8-0.3}$	3.21%	< 8.2	< 5.2
$D^+ \rightarrow K^+ \mu^+ \mu^-$	$2.9^{+8.0+0.2}_{-7.0-3.7}$	0.75%	< 22.2	< 14.0
$D^+ \rightarrow K^+ e^+ \mu^-$	$-3.4^{+6.5+1.0}_{-5.6-0.1}$	1.64%	< 5.7	< 3.6
$D^+ \rightarrow K^+ \mu^+ e^-$	$-4.4^{+7.1+1.4}_{-6.1-3.0}$	1.64%	< 5.9	< 3.7
$D_s^+ \rightarrow K^+ e^+ e^-$	$-3.8^{+6.2+1.5}_{-5.3-1.3}$	2.81%	< 1.8	< 6.6
$D_s^+ \rightarrow K^+ \mu^+ \mu^-$	$5.0^{+6.5+0.1}_{-6.1-0.3}$	0.68%	< 7.1	< 25.4
$D_s^+ \rightarrow K^+ e^+ \mu^-$	$-3.7^{+5.1+1.4}_{-4.4-1.4}$	1.40%	< 1.5	< 5.6
$D_s^+ \rightarrow K^+ \mu^+ e^-$	$-6.5^{+4.9+0.2}_{-4.3-1.1}$	1.40%	< 1.0	< 3.6
$\Lambda_c^+ \rightarrow p e^+ e^-$	$0.9^{+4.1+0.4}_{-3.4-0.1}$	4.11%	< 0.7	< 3.6
$\Lambda_c^+ \rightarrow p \mu^+ \mu^-$	$6.9^{+4.7+0.3}_{-3.7-0.6}$	0.67%	< 8.1	< 40.4
$\Lambda_c^+ \rightarrow p e^+ \mu^-$	$0.2^{+2.9+0.5}_{-2.0-0.5}$	1.19%	< 1.8	< 8.9
$\Lambda_c^+ \rightarrow p \mu^+ e^-$	$-0.2^{+2.5+0.5}_{-1.7-0.9}$	1.18%	< 1.5	< 7.5

Table 5: Yields from fits to the $D_{(s)}^+ \rightarrow \pi^+ \phi_{\ell^+ \ell^-}$ candidates. The first error is statistical and the second is the systematic error on the yield. The third column is the branching fraction for $\phi \rightarrow \ell^+ \ell^-$ calculated by normalizing to the $D_{(s)}^+ \rightarrow \pi^+ \phi_{KK}$ decay modes. The fourth column is the significance of the signal.

Decay mode	Yield (events)	Efficiency	BF($\phi \rightarrow \ell^+ \ell^-$) (10^{-4})	Significance
$D^+ \rightarrow \pi^+ \phi_{e^+ e^-}$	$19.0^{+7.1+0.4}_{-5.9-2.9}$	4.11%	$3.9^{+1.5+0.2}_{-1.2-0.6}$	2.7σ
$D^+ \rightarrow \pi^+ \phi_{\mu^+ \mu^-}$	$1.8^{+4.5+0.1}_{-3.7-0.7}$	0.67%	< 8.2 at 90% CL	0.3σ
$D_s^+ \rightarrow \pi^+ \phi_{e^+ e^-}$	$50.5^{+9.0+1.6}_{-8.1-3.9}$	1.19%	$2.8^{+0.5+0.2}_{-0.5-0.3}$	6.8σ
$D_s^+ \rightarrow \pi^+ \phi_{\mu^+ \mu^-}$	$15.3^{+6.1+1.3}_{-4.8-0.3}$	1.18%	$3.5^{+1.4+0.4}_{-1.1-0.2}$	3.2σ

References

- [1] T. Hurth, Rev. Mod. Phys. **75**, 1159 (2003).
- [2] G. Burdman, E. Golowich, J. Hewett and S. Pakvasa, Phys. Rev. D **66**, 014009 (2002).
- [3] S. Fajfer, S. Prelovsek and P. Singer, Phys. Rev. D **64**, 114009 (2001).
- [4] G. Burdman, E. Golowich, J. Hewett and S. Pakvasa, Phys. Rev. D **52**, 6383 (1995).
- [5] S. Fajfer and S. Prelovsek, Phys. Rev. D **73**, 054026 (2006).
- [6] B. Aubert *et al.* (BABAR Collaboration), Phys. Rev. Lett. **93**, 191801 (2004).
- [7] Q. He *et al.* (CLEO-c Collaboration), Phys. Rev. Lett. **95**, 221802 (2005).
- [8] D. Buchholz *et al.* (D0 Collaboration), Contribution to FPCP2006, hep-ex/0605090.
- [9] J. M. Link *et al.* (FOCUS Collaboration), Phys. Lett. B **573**, 21 (2003).
- [10] E. M. Aitala *et al.* (E791 Collaboration), Phys. Lett. B **462**, 401 (1999);
K. Kodama *et al.* (E653 Collaboration), Phys. Lett. B **345**, 85 (1995).
- [11] S. Eidelman *et al.* (Particle Data Group), Phys. Lett. B **592**, 1 (2004).
- [12] B. Aubert *et al.* (BABAR Collaboration), Nucl. Instr. Methods Phys. Res., Sect. A **479**, 1 (2002).
- [13] D. J. Lange, Nucl. Instr. Methods Phys. Res., Sect. A **462**, 152 (2001).
- [14] S. Agostinelli *et al.* (GEANT4 Collaboration), Nucl. Instr. Methods Phys. Res., Sect. A **506**, 250 (2003).
- [15] J. D. Bjorken and S. J. Brodsky, Phys. Rev. D **1**, 1416 (1970).
- [16] T. Skwarnicki (Crystal Ball Collaboration), Ph.D. thesis, Cracow Institute of Nuclear Physics (1986), DESY-F31-86-02.